# A highly stable, pressure-driven, flow control system based on Coriolis mass flow sensors for organs-on-chips

de Haan, Pim; Mulder, Jean Paul S.H.; Lötters, Joost C.; Verpoorte, Elisabeth

**DOI**
10.1016/j.flowmeasinst.2024.102576

**Publication date**
2024

**Document Version**
Final published version

**Published in**
Flow Measurement and Instrumentation

**Citation (APA)**
de Haan, P., Mulder, J. P. S. H., Lötters, J. C., & Verpoorte, E. (2024). A highly stable, pressure-driven, flow control system based on Coriolis mass flow sensors for organs-on-chips. *Flow Measurement and Instrumentation*, *97*, Article 102576. https://doi.org/10.1016/j.flowmeasinst.2024.102576

Flow Measurement and Instrumentation 97 (2024) 102576

Contents lists available at ScienceDirect

Flow Measurement and Instrumentation

journal homepage: www.elsevier.com/locate/flowmeasinst

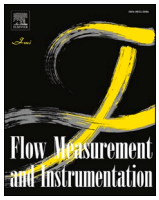

# A highly stable, pressure-driven, flow control system based on Coriolis mass flow sensors for organs-on-chips

Pim de Haan [a,b], Jean-Paul S.H. Mulder [a], Joost C. Lötters [c,d,e], Elisabeth Verpoorte [a,*]

[a] University of Groningen, Groningen Research Institute of Pharmacy, Pharmaceutical Analysis, Antonius Deusinglaan 1, 9713 AV, Groningen, the Netherlands
[b] TI-COAST, Science Park 904, 1098 XH, Amsterdam, the Netherlands
[c] Bronkhorst High-Tech B.V., Nijverheidsstraat 1A, 7261 AK, Ruurlo, the Netherlands
[d] University of Twente, MESA+ Institute for Nanotechnology, P.O. Box 217, 7500 AE, Enschede, the Netherlands
[e] Delft University of Technology, Department of Precision and Microsystems Engineering, Mekelweg 2, 2628 CD, Delft, the Netherlands

ARTICLE INFO

*Keywords:*
Flow control system
Coriolis flow sensor
Organ-on-a-chip
Flow stability

ABSTRACT

Stable delivery of liquids to microfluidic systems is essential for their reproducible functioning, especially when supplying flows to organs-on-chips – delicate living models that recreate human physiology on the microscale and thus can be used to reduce the need for animal testing. Most flow control systems are unable to sustain a robust and stable flow in longer experiments (>1 week), particularly those based on the ubiquitous syringe pump. Though easy to use, syringe pumps have no mechanism for actually measuring flow, let alone flow regulation with sensor feedback. We have developed a liquid delivery system based on the generation of flow by applying a constant air pressure to liquids in sealed containers. A flow of liquid is monitored by accurate measurement of mass flows (mg/min) using downstream Coriolis-based mass flow sensors. Measured mass flows provide fast feedback to integrated valves, with valves opening or closing slightly to increase or decrease solution flows to the organs-on-chips as required. This mass flow sensing principle is not affected by changes in the density, temperature, and viscosity of the liquids being displaced. This is in contrast to systems that use volumetric flow sensors, which require recalibration when these parameters change. The rationale behind using this principle for organs-on-chips, is that the stability provided by this flow control system allows for more control over growth of these mini-organs. We demonstrate the functionality of this system with three examples: 1) Fast stabilization (within seconds) under changing physical conditions; 2) Short-term stability (minutes to hours) of delivered flows in a microreactor with interconnected inlets; and 3) Long-term stability (>1 week) of cell medium flows to a living organ-on-a-chip. Two categories of organs-on-chips (OOCs) can be distinguished: 1) solid OOC are designed for three-dimensional cell or tissue constructs that interact with each other and their surroundings, and 2) barrier-type OOC contain a selective cellular barrier between two compartments as do many barriers in the body. The latter of these two types is the most challenging to culture and maintain as they are very sensitive to variations in flow and pressure surges. The flow control system presented in this work provides a great improvement compared to the use of syringe pumps and volumetric flow sensors in OOC studies. The novelty of this work lies in the long-term stability use of this system for organs-on-chips, maintaining stability for short to very long periods of time without compromising the barrier function of the organ-on-chip by pressure surges, bacterial contamination, or other undesired effects from the flow delivery system.

## 1. Introduction

Many different human biological tissues, both engineered and primary, have formed the basis of organ-on-a-chip (OOC) developments over the past decade, with the aim to mimic the physiological functions taking place in the human body. The organ-on-a-chip concept has, for example, emerged as a promising approach or tool to replace animal testing when studying medicinal drugs, in the context of drug development or in personalized medicine applications [1]. Reported OOC include a lung-on-a-chip [2], gut-on-a-chip [3], and many other single organs, with multi-organ-systems recently receiving growing attention [4–7]. Two categories of organs-on-chips (OOCs) can be distinguished:

* Corresponding author.
*E-mail address:* e.m.j.verpoorte@rug.nl (E. Verpoorte).

https://doi.org/10.1016/j.flowmeasinst.2024.102576
Received 23 June 2023; Received in revised form 6 March 2024; Accepted 7 March 2024
Available online 8 March 2024

1) solid OOC are designed for three-dimensional cell or tissue constructs that interact with each other and their surroundings, and 2) barrier-type OOC contain a selective cellular barrier between two compartments as do many barriers in the body [1]. In order to keep the cells or tissues inside these organ-chips thriving, they must be supplied continuously with medium containing nutrients and oxygen, and products of their metabolism must be removed. Given the necessity to emulate *in vivo* conditions [8,9], selection of the flow control system should not be underestimated, and a wide variety of options is available [10,11]. In delivering flows to OOC, it is essential to be able to modulate a stable, continuous supply of cell medium throughout the experiment. For barrier-type OOC, controlled shear stress exerted by the flow over the surface of the growing cells to mimic physiological shear stress is needed in many cases to make the cells behave like they do *in vivo*. Stable flow must often be regulated for days. For example, constant low flow rates result in the formation of villus- and crypt-like structures in Caco2-cell-based models of the human intestine after 5 days when cultured on a porous membrane that is peristaltically actuated. Under static conditions this process typically takes significantly longer, up to 21 days [12]. Flows of medium should therefore be stable, regulated for days to multiple weeks. Interruptions in the flow of medium can cause cells to deplete the medium of nutrients, as well as result in the accumulation of cellular waste products. Besides this, any temporary disconnection of the OOC from medium supply (e.g. to replace empty medium reservoirs) may have detrimental effects on the growing OOC culture. For instance, reconnection of the OOC to medium supply may lead to the formation of air bubbles, whose surface tension can destroy cell layers at the microscale. Microbial contamination may also occur, a situation that can lead to microbes outcompeting human cells in terms of proliferation, with the subsequent failure of the OOC as organ or disease model [1].

The different media used can be quite varied as a result of added biomolecular species, such as serum. Microfluidic techniques allow for the manipulation of nanoliter/min to milliliter/min flows, through networks of submillimeter-sized channels in organ-chips. However, controlled fluid flows may be difficult to achieve when the fluids involved are more physiological in nature, especially if the medium composition is to be changed over time to assess longer-term effects.

To date, syringe pumps are the most commonly used method to deliver cell culture medium to OOC systems, and they generally do so by so-called positive displacement. To achieve this, an internal stepper motor drives a belt, which connects to a drive screw, to which in turn the plunger of the liquid-loaded syringe is connected [13,14]. The syringe is slowly emptied as the plunger is pushed stepwise through the barrel of the syringe, transforming the linear velocity of the plunger to a volumetric flow. Since stepper motors have a fixed set of steps per cycle, low linear velocities will result in the pulsatile motion of the plunger in the syringe, causing the liquid flow to be non-constant (or pulsatile) [13].

Furthermore, the rotating spindle that couples the stepper motor to the syringe plunger is never completely cylindrical, which is also hypothesized to contribute to flow pulsations. In longer organ-on-a-chip experiments, for example, unpredicted flow pulsations are undesirable, as the cells or tissues in these living models may be highly susceptible to variations in the flow conditions. The OOC may be damaged beyond repair even by disconnecting the pump to simply exchange or refill the syringe. At any given volumetric flow rate, the use of narrower syringe barrels leads to a less pulsatile flow than wider barrels, because a higher plunger velocity is required. However, narrow syringe barrels would mean smaller barrel volumes as well, thereby reducing the time that flow can be sustained without switching syringes or otherwise refilling them. When using syringe pumps, a compromise is therefore necessary: narrower syringes lead to more stable flow, but also to shorter experiment times due to the reduced volumes of these syringes. A syringe pump therefore cannot sustain pulsation-free low flows in longer-term experiments. Moreover, the flows that are actually delivered by syringe pumps are not usually measured. It is often simply assumed that the syringe pump delivers its flow as programmed, even under changing conditions with respect to back pressure due to e.g. varying viscosity, or growth of biological material inside the channels.

Needless to say, fluctuating flow rates delivered by syringe pumps are undesirable when working with OOC. A pumping system that includes a flow sensor to monitor flow rates is a good first step. Better still is a flow sensor combined with a flow regulation component to allow not only monitoring of flow rates, but also active regulation of flow rates. In an effort to provide continuous pulsation-free flow over longer periods of time using larger volume reservoirs, we have developed a pressure-driven system using compressed gas to pressurize containers containing the liquids to be displaced. In our flow control system (Fig. 1), we employ five mass flow controllers with integrated valves, to regulate up to five flows of liquids independently of each other. The valves are piezoelectric proportional-control valves that are regulated by PID (proportional-integrative-derivative) controllers in the software to be more or less open. Just how large the mass flow is through one of these valves, is determined by the feedback signal provided by the mass flow sensor. While these mass flow controllers are well described in the literature, their application in OOC systems is new. The novelty of this work lies in the long-term use of this system for organs-on-chips, maintaining stability for short to very long periods of time without compromising the barrier function of the OOC by pressure surges, bacterial contamination, or other undesired effects from the flow delivery system. Even though one of the two types of mass flow sensors has recently become commercially available, the version that is available is used solely as flow *sensor*, i.e., without integrated valves to regulate flow [15]. Rather, the commercially available apparatus is equipped to regulate the magnitude of the delivered flow by precise control of the headspace pressure in the container. Our set-up uses an overpressure in the headspace, which eliminates the need for high-resolution (sub--mbar) pressure regulators.

The accurate delivery of flows depends both on the flow sensor itself, and its feedback control of the regulating valve. As flow sensors, we chose the most accurate flow sensors that are available. Mass flow sensors based on measurement of Coriolis force were integrated into the system to very precisely control flow rates (Fig. 1). To prevent gas bubbles in the liquid flow, the overpressure should be kept as low as possible (at ca. 500 mbar in our case). A flow of liquid is generated from the pressurized containers by displacement of liquid toward the downstream flow sensors [16]. The liquid subsequently flows through the rectangular tube of the Coriolis flow sensor, which is actuated with a frequency, $\omega$, in a torsional mode (Fig. 2). The inertia of the mass flowing through the tube in combination with its actuated vibration results in a Coriolis force, $F_c$. The Coriolis force leads to an induced out-of-plane vibration, which is detected by capacitive pick-up elements integrated in the Coriolis sensors. The Coriolis force is proportional to the mass flow, $\Phi_m$ [16], where $L$ is the length of the tube along the side of the rectangle opposite to the sensor inlet:

$$\overrightarrow{F_c} = -2 \cdot L \cdot (\omega \times \Phi_m) \tag{1}$$

The Coriolis sensing mechanism is independent of temperature, applied pressure and viscosity and may be applied across a wide range of mass flow rates for both liquids and gases (from less than 100 μg/min (microsensors) up to more than 1,000 kg/min, depending on flow sensor architecture) [17]. This is in contrast to the most commonly used thermal flow rate sensors in microfluidics, which measure volumetric flow rates by heating a small amount of liquid, and subsequently detecting the rate of heat dissipation using a downstream heat sensor [18]. These thermal sensors have a small working range, and their accuracy depends on liquid properties and the flow rate itself [19]. While thermal flow sensors have an accuracy of about 5% at the higher end of their range, the heat dissipates more extensively at lower flow rates since there is more time between the heating element and the heat sensor. Thermal sensors therefore suffer from a far poorer accuracy at the lower flow rate

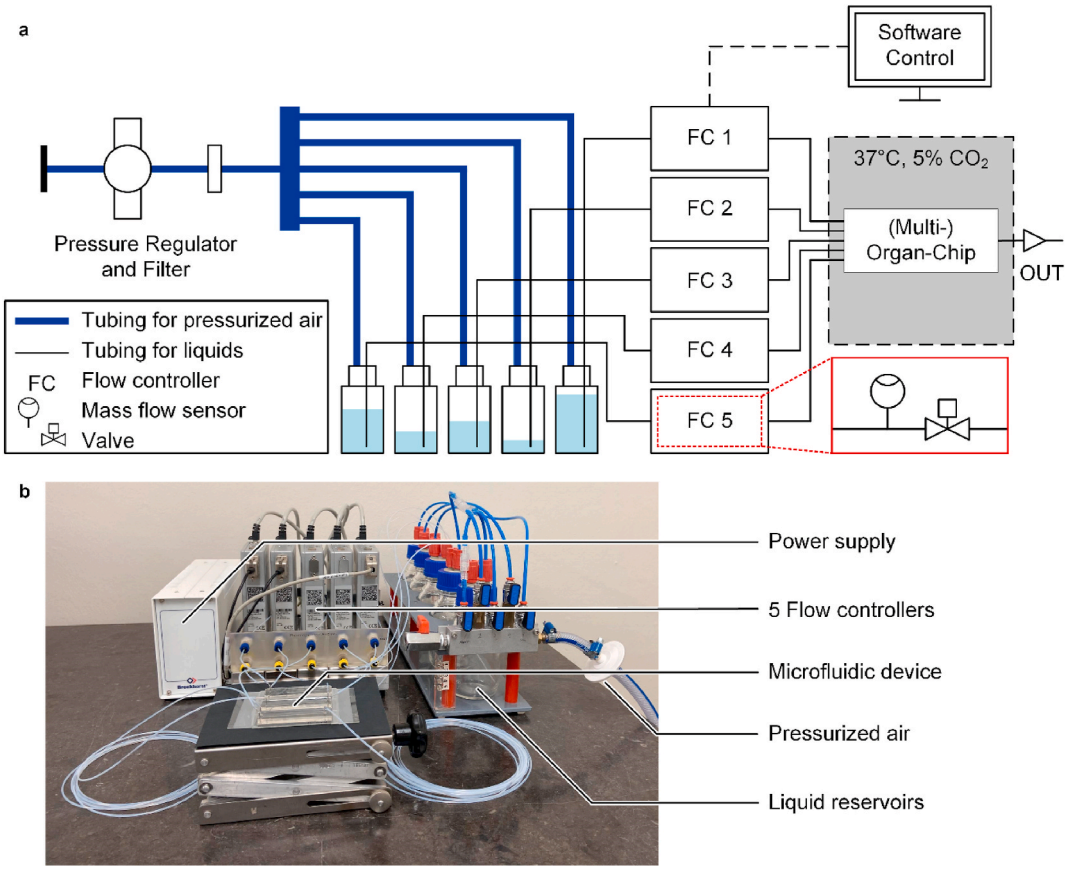


**Fig. 1.** **(a)** Schematic of the liquid delivery system. Pressurized air (top left) is connected to the five liquid reservoirs, to cause a pressure-driven flow toward the five flow controllers (FC). Each FC comprises a Coriolis-based mass flow sensor and a proportional control valve, as schematically shown in flow controller 5, after which the liquids flow to the multi-organ-chip in an incubator. **(b)** Photograph of the entire flow control system.

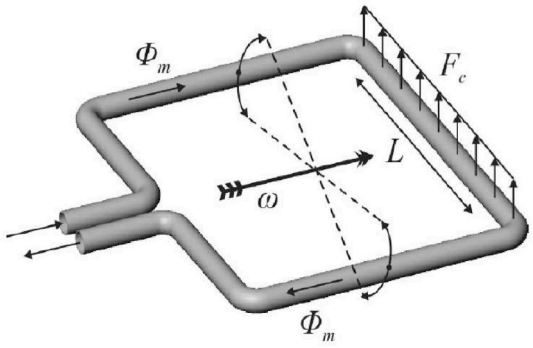


**Fig. 2.** The Coriolis-based mass flow sensor consists of a rectangular tube, which carries a mass flow $\Phi_m$. The tube vibrates in a torsional mode (ω) around the axis indicated by the center arrow. A Coriolis force, $F_c$, is detected along length L. Reproduced from Ref. [20] under a Creative Commons Attribution license.

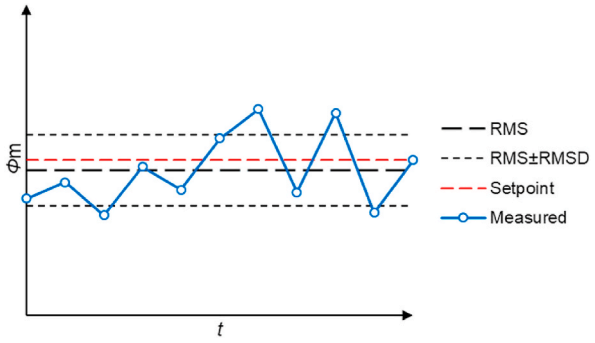


**Fig. 3.** Graphical depiction of flow accuracy and flow stability as these terms are used in this paper. Flow accuracy is a measure for the closeness of the delivered flows to the setpoint, and is calculated as root mean square (RMS) of the delivered mass flows over time. Flow stability, on the other hand, is the deviation of the measured mass flows around the average; and is calculated as root mean square deviation (RMSD). Flow stability is thus used in the same sense as the term 'precision' for other analytical instruments.

end of their useful range.

The aim of this work was to develop an accurate liquid delivery system for organs-on-chips, and demonstrate its stability in long-term experiments. Flow accuracy is defined as the closeness of the delivered mass flows to the setpoint (Fig. 3). It can be measured by calculating the quadratic mean (root mean square, or RMS) of the measured mass flow values over time. Flow stability is defined in terms of the minimal deviation from the mass flow setpoint. This can be measured by calculating the closeness of the measured mass flow values to their own average (root mean square deviation, or RMSD), and is thus a measure of analytical instrument precision. (The equations for calculating both RMS and RMSD are both presented in Section 4.3 below). We demonstrate the versatility of our system with three test cases. Case 1 involves fast stabilization (within seconds) under changing conditions, demonstrated by the mixing of water and ethanol at different ratios. This case is characterized by changing viscosity and density of the mixture depending on the water and ethanol fractions. Case 2 considers short-term stability (hours) of delivered flows to a multi-inlet, interconnected and interdependent microreactor. In Case 3, the long-term

(days) stability of the supply of cell culture medium to an OOC model system is monitored. Stable and continuous medium supply is of paramount importance in such cell cultures. If the supply were interrupted for as little as 1 h, chances are the cells would be damaged and die. We show that the rapid feed-back loop between the Coriolis mass sensor and the flow-regulating valve is capable of maintaining flow stability in all three cases. The high long-term stability of our medium supply system is much sought after in the OOC field [11].

## 2. Results and discussion

### 2.1. System design and operation

After passing through a microfilter to maintain sterility, pressurized air was distributed to five glass bottles containing the liquids to be supplied to the OOC (Fig. 1). The lowest possible overpressure was used (usually ca. 0.5 bar (g)) to prevent dissolution of gas in the liquid, which could lead to gas bubble formation downstream. Since standardized GL-45 caps with connectors were used, glass bottles of any volume could be implemented. Plastic 15- or 50-mL sample tubes could be inserted into these bottles in cases where smaller liquid volumes are needed. Poly (tetrafluoroethylene) (PTFE) tubing was inserted through the cap to the very bottom of these containers (or sample tubes), and these led the liquids to one of the five mass flow controllers (FC) that form the heart of flow regulation. Two types of mass flow controllers were used in this system, each having a different flow range (Table 1). Two elements inside these flow controllers are shown in an insert in Fig. 1: a Coriolis-based mass flow sensor that very precisely determines the mass flow passing through it, independent of liquid parameters such as viscosity and density, and a proportional-control valve that is continuously adjusted based on feed-back information from the sensor. The Bronkhorst software package was employed to change flow controller settings, establish a simple flow rate program, and record measurements of mass flow and density (see Section 4: *Methods* for more details). The specific settings of the PID algorithm could be adjusted in the software as well, for example to more aggressively adjust flows to the setpoint (with the risk of overshooting), or more subtly change the flow rate at the cost of slower settling. The settling time resulting from flow rate adjustment depends on this specific setting, as well as liquid properties (viscosity, density) and the magnitude of the set flow rate.

Two different microfluidic systems were used to characterize the performance of the flow system. So-called 'chaotic' micromixers, microchannels containing grooves arrays to perturb flows under laminar-flow conditions, were used to enhance mixing in microchannels [21,22]. These mixers had channel lengths of 51.5 mm and an internal volume of only 1.38 μL. In Case 1, the mixing process of ethanol and water was studied in a single grooved micromixer. This example was chosen specifically because binary ethanol/water mixtures have varying densities (increasing with the water content) and varying (non-linear) viscosities. For Case 2, three micromixers were connected in series to emulate the digestive functions of the gastrointestinal tract and to study the stability of flows in an interconnected and interdependent microreactor [23,24]. In Case 3, the organ-on-a-chip experiment, a gut-on-a-chip device with two 150-μm-deep channels, aligned vertically with one channel directly over the other, was used. These channels were separated by a homemade 30-μm-thick poly(dimethylsiloxane) membrane, with Caco-2 BBE intestinal epithelial cells grown on top.

**Table 1**
Two types of flow controllers (Bronkhorst High-Tech, Ruurlo, the Netherlands) were used in the liquid delivery system, having different flow ranges. Zero stability is the accuracy at very low flows.

| | Mini-Flow Controller | Micro-Flow Controller |
|---|---|---|
| Type number | ML120 | BL100 |
| Number present in system | 3 | 2 |
| Flow range | 0.05–200 g/h | 0.01–2 g/h |
| Nominal accuracy | ±0.2% of reading ± zero stability | ±0.5% of reading ± zero stability |
| Zero stability | 0.010 g/h | 0.002 g/h |
| Density accuracy | ±5 kg/m$^3$ | ±5 kg/m$^3$ |

### 2.2. Cleaning and sterilization

As opposed to pumps based on plastic syringes, which exclusively have disposable parts in contact with the liquid to be pumped, our flow system is non-disposable and thus requires regular cleaning and sterilization. The limiting factor for sterilization is the internal material of the flow controller, since this material may be susceptible to chemical degradation. Wetted materials of the micro-flow controller (BL100) are stainless steel, perfluoroelastomer (Kalrez) and silicon nitride; the wetted material of the mini-flow controller (ML120) is stainless steel only. While perfluoroelastomer and silicon nitride are very inert, stainless steel is susceptible to strongly corrosive liquids, and therefore strong acids and sodium hypochlorite (a commonly used disinfectant) cannot be used. In our flow control system, we used 70% ethanol (Boom, Meppel, the Netherlands) in water (at a highest flow rate of 200 g/h for the ML120 or 2 g/h for the BL100, for at least 30 min) to sterilize the tubing and the internal volume of the flow sensors before any experiment involving living cells, after which the system was flushed with sterile water (ultrapure water, autoclaved at 121 °C for 20 min). Possible protein fouling was removed using a 0.1% sodium dodecyl sulfate (SDS, Acros, Geel, Belgium) solution in water at the highest flow rate used for the sensor in question, for at least 30 min. The system was then flushed with ultrapure water for at least 3 h, and sterilized as described above.

### 2.3. Case 1 – Fast stabilization under changing conditions: mixing water and ethanol

Absolute ethanol and water were mixed at different ratios in a micromixer, with the total mass flow rate constant at 100 mg/min (Fig. 4B), to study the stability of the generated flows under changing physical conditions such as density, viscosity, and the volumetric flow rate. While the mass flow rates were kept constant at 100 mg/min, the densities of ethanol and water differ significantly (786 kg/m$^3$ and 997 kg/m$^3$, resp., at 25 °C), leading to a changing volumetric flow rate (Fig. 4C). The density of the effluent ethanol/water mixture was measured by a third flow sensor (Fig. 4D), which only exhibited a brief delay with respect to Fig. 4B that was caused by the internal volume of the micromixer (1.38 μL) and the tubing leading from the micromixer into the flow sensor. The changing volumetric flow rates did not lead to any visible deviation in the mass flow rates or the stability of the flows (Fig. 4B and C). The viscosity of the ethanol/water mixture changed as well, since the viscosity of 50% ethanol (v/v in water, or ethanol mole fraction ~0.24) is 2.39 MPa•s, which is more than two times higher than that of pure water (0.89 MPa•s) or pure ethanol (1.10 MPa•s) [25]. This changed viscosity also had no visible effect on the stability of the flows, in contrast to systems relying on volumetric flow rates. Finally, we plotted the measured density versus the mole fraction of ethanol in the mixture (Fig. 4E), and we found a relation very similar to that reported in the literature [25].

Coriolis-based flow sensors have a great advantage when measuring the properties of a flow that varies during an experiment, as they do not need to be calibrated for different solvents. Any mass flowing through the sensor will lead to a sensor signal. This makes this system perfect for handling complex biological liquid mixtures.

### 2.4. Case 2 – Short-term stability in interconnected microreactors: digestion-on-a-chip

A flow of the protein solution (lactoferrin in water) was mixed serially with saliva, gastric juice and intestinal juice in a continuous-flow

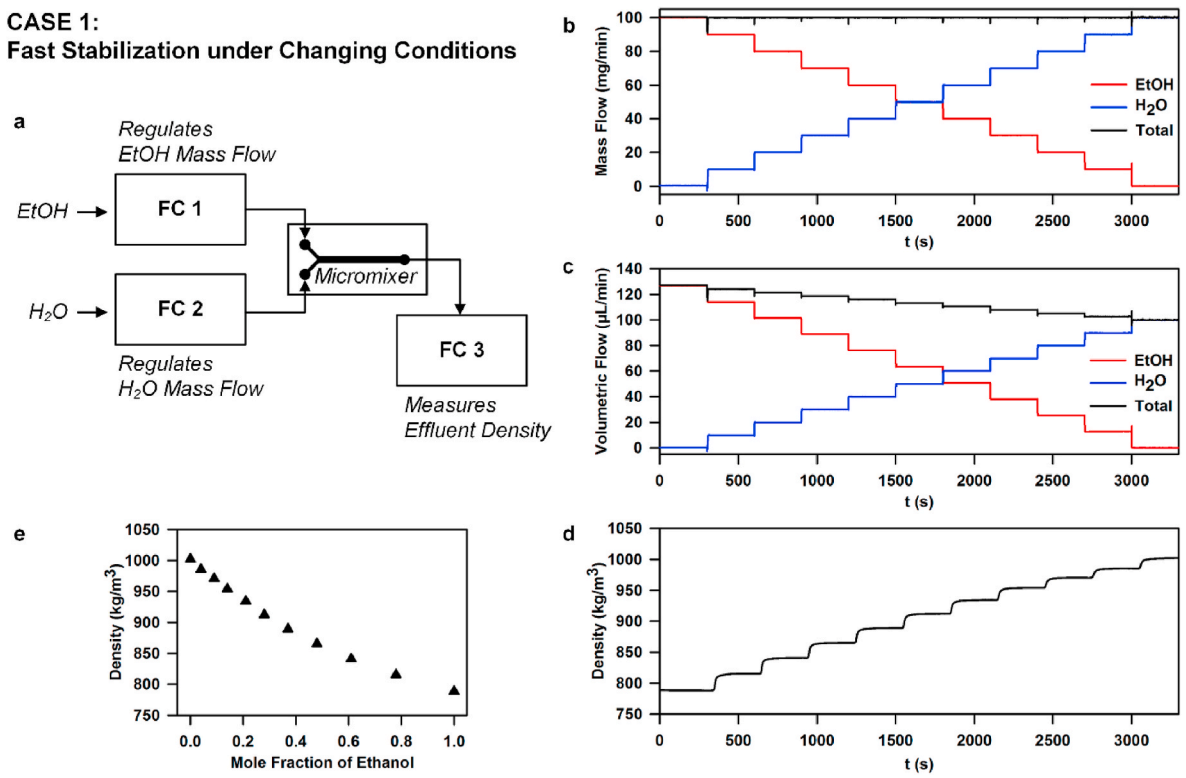


**Fig. 4.** Case 1: Fast stabilization under changing conditions. **(a)** Mass flows of absolute ethanol and ultrapure water were generated by FC 1 and 2. These were programmed to change the mass ratio of ethanol to water inside the micromixer every 300 s in increments of 10 mg/min. Flow controller 3 downstream of the micromixer only measured the density of the effluent mixture, without influencing the flow (valve fully open). **(b)** Measured mass flow rates of ethanol and water (mg/min), and the sum of these two, plotted versus the experiment time. **(c)** The corresponding volumetric flow rates (µL/min) were calculated from the mass flow rates and the density measured by FC 3, and plotted versus the experiment time. **(d)** The density of the effluent (kg/m$^3$) was measured, and plotted versus time to show the incremental increase when more water was added to the mixture. **(e)** The average density of water–ethanol mixtures (kg/m$^3$) was measured over 100 s in each of the steps in this experiment, and plotted versus the fraction of ethanol in the solvent mixture.

system to allow the digestive enzymes contained in these artificial juices to work. Loops after each microreactor were employed to increase the incubation times to approach values consistent with the human digestive system. Each microreactor consisted of two inlet channels merging in a main channel, incorporating microgrooves. The two flows were perturbed by these microgrooves, which greatly enhances mixing in this laminar-flow regime [21]. Since each stage of the digestive process was recreated in a separate microreactor, it was necessary to control these inlet flows individually, to keep the chemical environment (including local mineral composition and pH) constant, without affecting the processes downstream.

Table 2 shows the results of the stability measurements, calculated from the recorded flow data of a protein digestion experiment. The root mean square (RMS) of each of the signals represents the average output of each flow sensor, which is ideally identical to the setpoint. The RMS values were almost equal to each setpoint, indicating that the flow control system delivers flows as demanded by the setpoint. The stability of the flow system (here defined as the ability to deliver flows with as little variation as possible) was measured by determining the root mean square deviation (RMSD), monitoring the deviation of each individual measurement from the average measured signal.

The measured RMSD values were on the order of tens of micrograms per minute, indicating a very high stability. The normalized RMSD was below 1% for each of the flows, indicating the high stability of all flows. Moreover, the stability of these flows does not depend on the magnitude of the setpoint. The stability and performance of the mass flow sensors are independent of the flow rate, and other fluid properties such as viscosity and density. This is in contrast to thermal flow sensors, which are calibrated to measure the flow rate of a specific liquid (for example, pure water or pure isopropanol), under specified conditions such as fixed temperature. Thermal flow sensors are therefore dependent on the thermal properties of the solutions or liquid mixtures in which they are used, and should be calibrated for each new type of liquid mixture. The accuracy of the flow rate measurements achieved in this experiment would not have been possible with thermal flow sensors, as their accuracy depends on the thermal properties of the liquid.

The stability of the flows generated by the flow system was high, but it should be noted that these parameters were determined in the absence of external sources of flow variation. As the flow sensors contain a vibrating loop, which is affected by a mass flow passing through it, any external sources of vibration may also contribute to a changing signal. These sources could include other activities taking place on the same workbench (such as the opening or closing of incubator doors), or by someone touching any of the tubing connecting the flow system to the

**Table 2**
Analysis of flow data from digestion-on-a-chip experiments, performed as first described elsewhere [23]. The set-up and flow rates are described in Fig. 5.

| Liquid | Flow Controller | Setpoint (mg/min) | RMS (mg/min) | RMSD ( × $10^{-3}$ mg/min) | NRMSD (%) |
|---|---|---|---|---|---|
| Sample solution | Micro-Coriolis | 1.00 | 1.000024 | 6.75 | 0.67 |
| Saliva | Micro-Coriolis | 4.00 | 3.999719 | 3.88 | 0.10 |
| Gastric Juice | Mini-Coriolis | 8.00 | 8.000114 | 15.6 | 0.20 |
| Intestinal Juice | Mini-Coriolis | 12.00 | 12.00012 | 29.6 | 0.25 |

microfluidic set-up. To reduce these vibration effects, the flow controllers are attached to a massive block of stainless steel (2 kg each). The micro-Coriolis sensors operate at a higher vibration frequency and are therefore much less susceptible to external sources of vibration. Another source of variation is the occasional presence of gas bubbles in the flow streams, causing sharp and narrow peaks in the flow plots. The presence of gas, however, is a physiological phenomenon in digestive processes, and its presence does not lead to a disturbance of the flow patterns in our miniaturized system. The liquid containers were pressurized with the lowest possible air pressure, to minimize the amount of gas that dissolves in the liquid. Using other gases with a lower solubility (such as helium) or introducing a gas-impermeable barrier between the pressurizing gas and the liquid (a diaphragm or bellow) could further reduce the dissolution of gases in the liquid. This does not, however, eliminate gas originating from digestive processes (likely $CO_2$), but the flow controller will sense this as a sharp, short, drop in density.

### 2.5. Case 3 – Long-term stability: gut-on-a-chip

A gut-on-a-chip device, containing two overlapping microfluidic channels separated by a porous PDMS membrane as described above, was perfused with cell medium. The upper and lower channels of this device were perfused to supply the intestinal cells grown on top of the membrane with fresh nutrients. This required the use of two flow controllers in our flow control system, each associated with a microflow sensor. Fig. 6 shows a four-day plot for the flow in the top channel (containing the intestinal cells) and the bottom channel (without cells). The flow was set to 0.5 mg/min, which corresponds to a volumetric flow rate of 0.5 μL/min or a linear flow rate of 3.3 mm/min. The peaks just after t = 0 h indicate the positioning of the microfluidic device in the incubator. Other minor peaks throughout the flow plot are thought to arise from occasional air bubbles in the cell medium.

The peaks around t = 29 h in flow plots for both the top and bottom channels are expanded in the smaller insert graphs to the right of each flow plot. These peaks can be clearly annotated in the inserts. The first two peaks (red arrows) were caused by moving the device from and to the incubator for visual inspection with the microscope. The other peaks in each insert (blue arrows) were caused by briefly decreasing the flowrate first to 0.1 mg/min, then increasing it to 1.0 mg/min, before returning to 0.5 mg/min. This result indicates that the flow rates can be changed while the experiment is running, without causing a pressure surge in the device that could damage the cells. Flow rate stabilization is extremely rapid, on the order of just a few seconds. The results also show that the flow system is sensitive to external vibrations, for example when moving the set-up from the incubator to the microscope, but the recovery is almost immediate. This gut-on-a-chip was continuously perfused with medium for 11 consecutive days.

### 2.6. Strengths and limitations

The system described in this paper delivers flows of liquid to OOCs from a pressurized container, through a Coriolis-based mass flow sensor, and adjusted to a set mass flow rate by integrated valves. Many of the strengths of the set-up described in this study are inherent to using *mass* flow sensors, rather than *volumetric* flow sensors. The accuracy of the delivered flow is not dependent on the magnitude of the mass flow itself, which makes that the sensors are equally useful over a very wide flow rate range. The integrated control valves regulate the mass flow to the setpoint within seconds, with the exact settling time after adjustment depending on different factors (algorithm settings, liquid properties, and the set mass flow itself – see Materials and Methods). The choice to pressurize the headspace of the container (in this case, glass bottles) makes that the stored volume is nearly unlimited, in principle.

Limitations of the system are inherent to the Coriolis principle and the system design, too. The vibrations of the loop in the Coriolis sensor are measured and correlated to a mass flow, but external vibrations are registered as well and may affect the measurements (Fig. 6b, labeled 'Artefacts'). A heavy weight attached to the mass flow controllers mitigates this to some extent, but a solid, heavy table is preferred for optimal functioning of the sensors. The system requires quite some tubing to connect the reservoir to the flow controller, and then to the microfluidic chip; this makes the system unsuitable for the use of small volumes of liquids (e.g. <1 mL). Finally, as the headspace is pressurized with air, this may lead to dissolution of gases (nitrogen, oxygen) into the liquid being pumped. While this effect is minimized by using a relatively small overpressure, it must be taken into account e.g. when oxygen is not wanted in the system. In the case of organs-on-chips, oxygen is usually consumed by the living cells, but if this system were to be employed to perform chemical reactions, the extra oxygen may provide a problem (e.g. in oxidation-sensitive reactions). Choosing a different, inert gas may help in that case.

## 3. Conclusions

We have described the development of a highly stable liquid delivery system, consisting of pressurized liquid containers of virtually any size

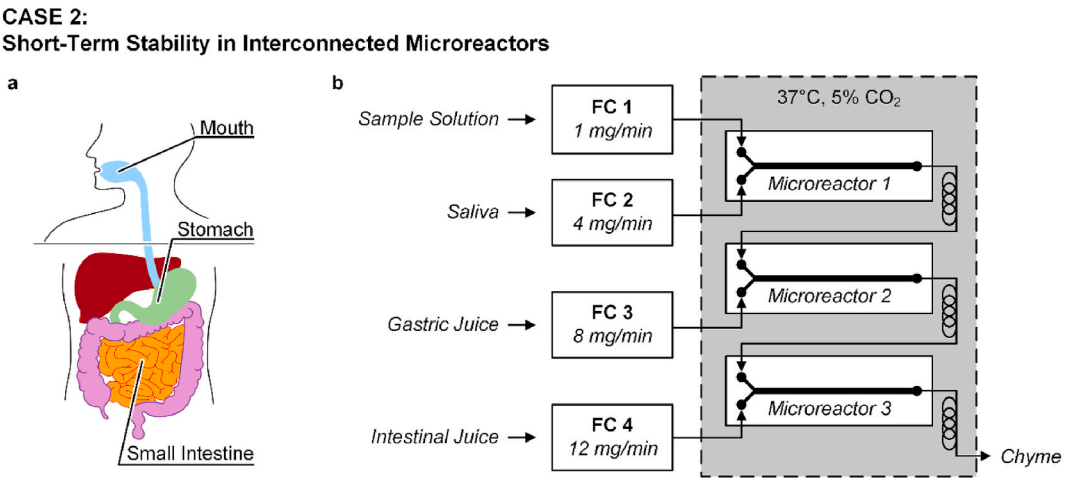


**Fig. 5.** Case 2: Short-term stability in interconnected microreactors. In this case, the flows in a digestion-on-a-chip experiment (performed according to a procedure reported earlier [23]) were studied to measure their stability. **(a)** The human gastrointestinal system, showing mouth, stomach, liver, and the small and large intestine. **(b)** The digestive system recreated in three flow-through microreactors, supplied with artificial digestive juices by four Coriolis-based mass flow controllers. Image A: Courtesy of Meike van der Zande, Wageningen Food Safety Research, the Netherlands.

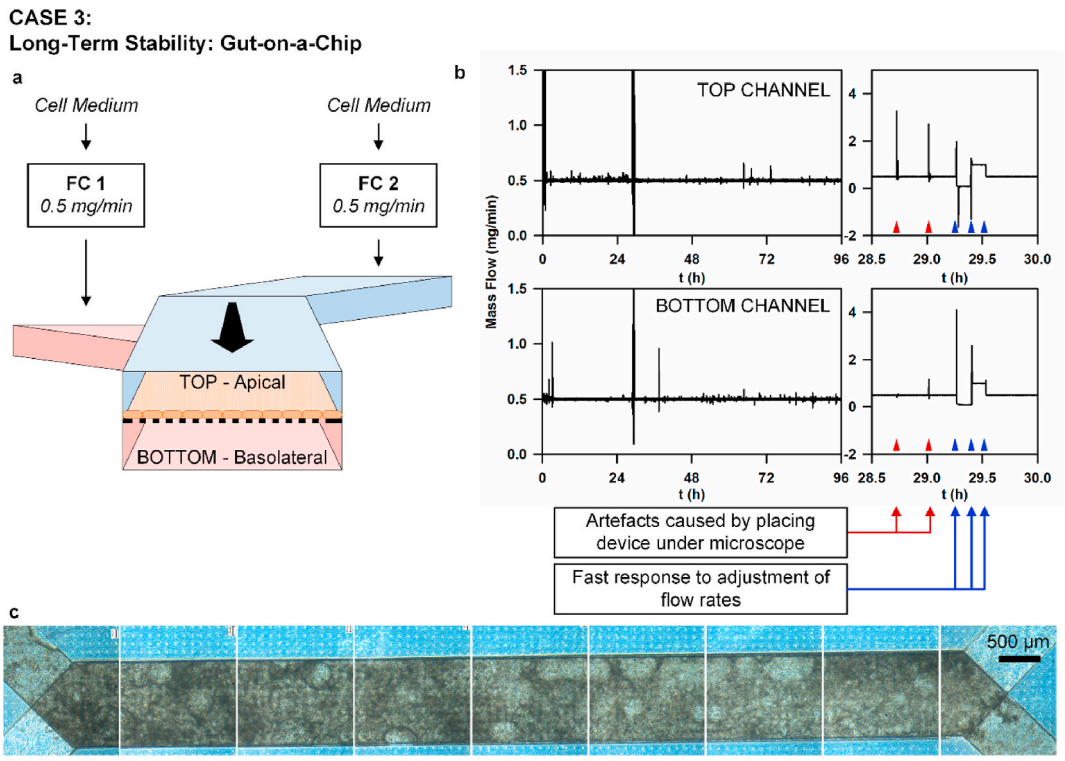


**Fig. 6.** Long-term stability, demonstrated by a sensitive organ-on-a-chip experiment. **(a)** Flow scheme of the gut-on-a-chip experiment, with two flow controllers supplying cell medium. **(b)** Left: Two four-day plots of the mass flow rates of medium delivered to the top and bottom channels of the device, set at 0.5 mg/min (corresponding to ~0.5 µL/min), indicating long-term stability at low flow rates. Inserts, upper right: The device was moved onto the microscope platform for visual inspection between 28.5 and 29 h (red arrows), with the motion sensed by the flow sensors causing a brief peak. Insert, lower right: Later, the flow rate was changed first to 0.1 mg/min and then 1.0 mg/min (blue arrows, ~0.1 µL/min and 1.0 µL/min, resp.). Clearly, flows stabilized rapidly after each change. **(c)** Phase-contrast micrographs of the living gut-on-a-chip (top view) after 11 days. As the volume of medium above the cells is limited (1.5 µL), these cells would have died if the flow of medium had faltered.

and flow controllers based on Coriolis mass flow sensors and proportional control valves. We have demonstrated that this mass flow system remains stable when using more complex biological liquids such as digestive juices, when supplying sensitive barrier-type organs-on-chips with fresh medium, and when using an ethanol/water mixture whose viscosity varies with the ratio of ethanol to water. With RMS and NRMSD well below 1% of the measured signal, the delivered flows are highly stable, making this system well suited for use in conjunction with both solid and barrier-type organs-on-chips. This constitutes a significant innovation in flow delivery for OOC when compared to both syringe pumps, which deliver a flow that is not measured at all, and thermal flow sensors, which have a quite low accuracy that gets worse at the lower end of their range. The feedback incorporated in the system continuously and quickly corrects the delivered flow to the setpoint, thereby ensuring a stable flow for extended times. Our system would also be very suited to use with microfluidic flow chemistry platforms, in which the product of chemical reactions could dramatically change liquid composition. The density of each flow is continuously measured, which provides additional information on processes taking place in the system. The Coriolis-based sensing of mass flow is independent of liquid properties, such as density and viscosity, and the system could be used for over 11 days.

## 4. Methods

All chemicals were obtained from Sigma-Aldrich/Merck (Zwijndrecht, the Netherlands), unless stated otherwise. Ultrapure water (18.2 MΩ•cm) was used to prepare all aqueous solutions. Microfluidic devices were fabricated by micromolding, by pouring PDMS (Sylgard 184, Dow Corning, Midland, MI, USA) over micromolds that were fabricated in-house (SU-8 negative photoresist on glass wafers) [26]. The fabrication of flexible PDMS membranes with 12 µm pores using SU-8 molds is described elsewhere [27].

### 4.1. System design and operation

The in-house wall outlet was connected to a pressure regulator (1 bar (g), Messer Griesheim, Bad Soden, Germany), and pressurized air was led to each of the five containers (Duran Protect with GL-45 standardized thread, 250 mL or 500 mL, Mainz, Germany) after passing through a microfilter (PTFE, 0.45 µm pores, Boom, Meppel, the Netherlands) to remove any particles or microbial contamination. The liquid in each of the containers is kept at a constant pressure (ca. 500 mbar (g) to prevent dissolution of gas in the liquid, which could lead to gas bubble formation downstream). Each container could be disconnected from the pressure supply individually (for example, if an exchange of medium was necessary). To minimize contamination, the bottles and caps were cleaned and sterilized by autoclaving, after which they were moved to an aseptic laminar air flow cabinet where they were filled with medium. When small volumes were required, the liquids were contained in a 15- or 50-mL plastic tube (Cellstar, Greiner Bio-One, Frickenhausen, Germany) inside the glass container. Poly(tetrafluoroethylene) (PTFE) tubing (0.8/1.6 mm inner/outer diameter, Polyfluor Plastics, Breda, the Netherlands) was used to allow the flow of liquids from their respective containers to the flow controllers (ML120 or BL100, Bronkhorst High-Tech, Ruurlo, the Netherlands, see Table 1), using blunt Fine-Ject 21G needles (Henke Sass Wolf, Tuttlingen, Germany) to connect the tubing. The same tubing was used to connect the flow controllers to the microfluidic devices. The Bronkhorst software package was employed to change flow controller settings and to record

measurements of mass flow and density.

### 4.2. Case 1 – Fast stabilization under changing conditions: mixing water and ethanol

Flows of absolute ethanol (VWR, Fontenay-sur-Bois, France) and ultrapure water were regulated by two mini-Coriolis flow controllers and led into a micromixer as described above (T = 25 °C). The flow rates were controlled by a customized flow program, which started at 100 mg/min ethanol and 0 mg/min water. The mass flow rates of ethanol and water were maintained for 5 min, after which they were changed in increments of −10 mg/min ethanol and +10 mg/min water and kept constant for 5 min. The concentration of ethanol in the mixture was decreased continuously in this way, and the concentration of water increased, to obtain pure water at the end of the experiment. A third mini-Coriolis flow sensor was used to measure the density of the effluent, which increases upon the addition of more water to the mixture, without influencing the flow (valve fully open). The outlet of the flow sensor was connected to a fluidic resistor (a needle bent at various places) to prevent the formation of gas bubbles. The density of the water/ethanol mixtures was averaged over a 100-*s*-period, and this was used to calculate the corresponding volumetric flow rates from mass flow rates.

### 4.3. Case 2 – Short-term stability in interconnected microreactors: digestion-on-a-chip

Flow stability was measured in digestion experiments in which the milk protein, lactoferrin (Vivinal, FrieslandCampina, Amersfoort, the Netherlands), was digested in our three-stage, miniaturized digestive system (Fig. 5B) [23,24]. Artificial digestive juices representing saliva, gastric juice, and intestinal juice were employed to mimic the biochemical conditions under which food is broken down. The system continuously mixes the sample (50 mg/mL lactoferrin in ultrapure water) with artificial saliva (in the mouth), then gastric juice (in the stomach), and intestinal juice (a 2:1 mixture of duodenal juice and bile, in the intestine), with the physiological ratios between these digestive juices represented by their relative flow rates. The composition of these juices is described elsewhere [23], but briefly each artificial juice is a physiological solution of minerals and enzymes in water, with the pH set such that it leads to *in vivo*-like conditions upon mixing with the other juices. The mass flow data from the last hour of digestion (33,023 datapoints) were analyzed to measure the stability of the flow controllers. The root mean square (RMS) of each channel was calculated from the mass flow over time:

$$RMS = \sqrt{\frac{1}{n}\sum_{i=1}^{n} x_i^2} \tag{2}$$

in these equations, $x_i$ represents every individual mass flow measurement (mg/min). The root mean square deviation (RMSD) of each channel was calculated from the mass flow over time, and was normalized as a percentage of the average flow:

$$RMSD = \sqrt{\frac{1}{n}\sum_{i=1}^{n} (x_i - \bar{x})^2} \tag{3}$$

$$NRMSD = \frac{RMSD}{\bar{x}} \bullet 100\% \tag{4}$$

In these equations, $\bar{x}$ represents the average mass flow (mg/min); NRMSD is the normalized RMSD.

### 4.4. Case 3 – Long-term stability: gut-on-a-chip

Caco-2 BBE intestinal epithelial cells (ATCC, Manassas, VA, USA) were grown in the top channel, on top of the membrane (surface area of the suspended part: 1 × 10 mm). Caco-2 BBE human intestinal cells were used between passages 52–54. Dulbecco's Modified Eagle Medium (DMEM, ThermoFisher, Waltham, MA, USA) supplemented with 25 mM glucose, GlutaMAX, 100 U/mL penicillin, 100 μg/mL streptomycin, 25 mM HEPES, and 10% fetal bovine serum (FBS) was the culture medium employed. Cells were seeded in T75 flasks (Greiner Bio-One) at 10,000 cells/cm$^2$, with the cells passaged at 70–90% confluency. The cells were detached from the flask by incubation with 3 mL of a 500 mg/L trypsin-200 mg/L EDTA solution (ThermoFisher) for 5 min, followed by centrifugation (1,000 rpm, 5 min). The supernatant was discarded and the cells were resuspended in fresh medium. For gut-on-a-chip experiments, the same culture medium was used, but supplemented with 20% FBS instead of 10%. The gut-on-a-chip devices were fabricated as described elsewhere [28], sterilized with 70% ethanol for at least 30 min and dried in a 60 °C oven. The two vertically aligned channels separated by the porous PDMS membrane were coated by filling them with a solution of collagen type I (50 μg/mL, ThermoFisher) and Matrigel (300 μg/mL, Corning, Corning, NY, USA) in DMEM (without any supplements) and incubating for 2 h without flow [3]. The channels were then washed with fresh culture medium containing all supplements (including 20% FBS), followed by cell seeding in the top channel at 150,000 cells/cm$^2$ under static conditions. After 2 h, cells had adhered to the coated membrane, and the flow of medium was started at 30 mg/h (corresponding to ~30 μL/h or 0.5 μL/min) in both channels.

## CRediT authorship contribution statement

**Pim de Haan:** Writing – review & editing, Writing – original draft, Validation, Methodology, Investigation, Formal analysis, Data curation, Conceptualization. **Jean-Paul S.H. Mulder:** Writing – review & editing, Methodology, Conceptualization. **Joost C. Lötters:** Writing – review & editing, Resources. **Elisabeth Verpoorte:** Writing – review & editing, Writing – original draft, Supervision, Funding acquisition, Conceptualization.

## Declaration of competing interest

The authors declare that they have no known competing financial interests or personal relationships that could have appeared to influence the work reported in this paper.

## Data availability

Data will be made available on request.

## Acknowledgements

This research received funding from the Dutch Research Council (NWO) in the framework of the Technology Area PTA-COAST3 (GUT-TEST, Project #053.21.116) of the Fund New Chemical Innovations.

## References

[1] C.M. Leung, P. de Haan, K. Ronaldson-Bouchard, G.-A. Kim, J. Ko, H.S. Rho, et al., A guide to the organ-on-a-chip, Nat Rev Methods Prim 2 (2022) 33, https://doi.org/10.1038/s43586-022-00118-6.

[2] D. Huh, B.D. Matthews, A. Mammoto, M. Montoya-Zavala, H.Y. Hsin, D.E. Ingber, Reconstituting organ-level lung functions on a chip, Science 328 (2010) 1662–1668, https://doi.org/10.1126/science.1188302.

[3] H.J. Kim, D. Huh, G. Hamilton, D.E. Ingber, Human gut-on-a-chip inhabited by microbial flora that experiences intestinal peristalsis-like motions and flow, Lab Chip 12 (2012) 2165–2174, https://doi.org/10.1039/c2lc40074j.

[4] P.M. van Midwoud, M.T. Merema, E. Verpoorte, G.M.M. Groothuis, A microfluidic approach for in vitro assessment of interorgan interactions in drug metabolism using intestinal and liver slices, Lab Chip 10 (2010) 2778–2786, https://doi.org/10.1039/c0lc00043d.

[5] P.G. Miller, M.L. Shuler, Design and demonstration of a pumpless 14 compartment microphysiological system, Biotechnol. Bioeng. 113 (2016) 2213–2227, https://doi.org/10.1002/bit.25989.
[6] T. Satoh, S. Sugiura, K. Shin, R. Onuki-Nagasaki, S. Ishida, K. Kikuchi, et al., A multi-throughput multi-organ-on-a-chip system on a plate formatted pneumatic pressure-driven medium circulation platform, Lab Chip 18 (2017) 115–125, https://doi.org/10.1039/c7lc00952f.
[7] J.H. Sung, J. Koo, M.L. Shuler, Mimicking the human physiology with microphysiological systems (MPS), BioChip J 13 (2019) 115–126, https://doi.org/10.1007/s13206-019-3201-z.
[8] G. Özkayar, J.C. Lötters, M. Tichem, M.K. Ghatkesar, Toward a modular, integrated, miniaturized, and portable microfluidic flow control architecture for organs-on-chips applications, Biomicrofluidics 16 (2022) 21302, https://doi.org/10.1063/5.0074156.
[9] H. Zhu, G. Özkayar, J. Lötters, M. Tichem, M.K. Ghatkesar, Portable and integrated microfluidic flow control system using off-the-shelf components towards organs-on-chip applications, 2022, https://doi.org/10.21203/rs.3.rs-2166950/v1.
[10] K. Kaarj, J.-Y. Yoon, Methods of delivering mechanical stimuli to organ-on-a-chip, Micromachines 10 (2019), https://doi.org/10.3390/mi10100700.
[11] C.K. Byun, K. Abi-Samra, Y.-K. Cho, S. Takayama, Pumps for microfluidic cell culture, Electrophoresis 35 (2014) 245–257, https://doi.org/10.1002/elps.201300205.
[12] H.J. Kim, D.E. Ingber, Gut-on-a-Chip microenvironment induces human intestinal cells to undergo villus differentiation, Integr. Biol. 5 (2013) 1130–1140, https://doi.org/10.1039/c3ib40126j.
[13] D. Alveringh, R.J. Wiegerink, J.C. Lötters, Towards system-level modeling and characterization of components for intravenous therapy, in: 2nd Int. Conf. Microfluid. Handl. Syst., 2014, pp. 106–109. Freiburg, Germany.
[14] J.R. Lake, K.C. Heyde, W.C. Ruder, Low-cost feedback-controlled syringe pressure pumps for microfluidics applications, PLoS One 12 (2017) 1–12, https://doi.org/10.1371/journal.pone.0175089.
[15] Elveflow Coriolis flow rate sensor. Paris, France. https://www.elveflow.com/microfluidic-products/microfluidics-flow-measurement-sensors/microfluidic-flow-sensor-coriolis/(accessed December 22, 2023).
[16] J. Haneveld, T.S.J. Lammerink, M.J. de Boer, R.G.P. Sanders, A. Mehendale, J. C. Lötters, et al., Modeling, design, fabrication and characterization of a micro Coriolis mass flow sensor, J. Micromech. Microeng. 20 (2010), https://doi.org/10.1088/0960-1317/20/12/125001.
[17] D. Alveringh, R.J. Wiegerink, J. Groenesteijn, R.G.P. Sanders, J.C. Lötters, Experimental analysis of thermomechanical noise in micro Coriolis mass flow sensors, Sensors Actuators, A Phys 271 (2018) 212–216, https://doi.org/10.1016/j.sna.2018.01.024.
[18] M.N.S. de Graaf, A. Vivas, A.D. van der Meer, C.L. Mummery, V.V. Orlova, Pressure-driven perfusion system to control, multiplex and recirculate cell culture medium for organs-on-chips, Micromachines 13 (2022), https://doi.org/10.3390/mi13081359.
[19] N.T. Nguyen, Micromachined flow sensors — a review, Flow Meas. Instrum. 8 (1997) 7–16.
[20] W. Sparreboom, J van de Geest, M. Katerberg, F. Postma, J. Haneveld, J. Groenesteijn, et al., Compact mass flow meter based on a micro coriolis flow sensor, Micromachines 4 (2013) 22–33, https://doi.org/10.3390/mi4010022.
[21] A.D. Stroock, S.K.W. Dertinger, A. Ajdari, I. Mezić, H.A. Stone, G.M. Whitesides, Chaotic mixer for microchannels, Science 295 (2002) 647–651, https://doi.org/10.1126/science.1066238.
[22] M.A. Ianovska, P.P.M.F.A. Mulder, E. Verpoorte, Development of small-volume, microfluidic chaotic mixers for future application in two-dimensional liquid chromatography, RSC Adv. 7 (2017) 9090–9099, https://doi.org/10.1039/C6RA28626G.
[23] P. de Haan, M.A. Ianovska, K. Mathwig, G.A.A. van Lieshout, V. Triantis, H. Bouwmeester, et al., Digestion-on-a-chip: a continuous-flow modular microsystem recreating enzymatic digestion in the gastrointestinal tract, Lab Chip 19 (2019) 1599–1609, https://doi.org/10.1039/c8lc01080c.
[24] P. de Haan, M.J.C. Santbergen, M. van der Zande, H. Bouwmeester, M.W.F. Nielen, E. Verpoorte, A versatile, compartmentalised gut-on-a-chip system for pharmacological and toxicological analyses, Sci. Rep. 11 (2021) 4920, https://doi.org/10.1038/s41598-021-84187-9.
[25] I.S. Khattab, F. Bandarkar, M.A.A. Fakhree, A. Jouyban, Density, viscosity, and surface tension of water+ethanol mixtures from 293 to 323K, Kor. J. Chem. Eng. 29 (2012) 812–817, https://doi.org/10.1007/s11814-011-0239-6.
[26] D.C. Duffy, J.C. McDonald, O.J.A. Schueller, G.M. Whitesides, Rapid prototyping of microfluidic systems in poly(dimethylsiloxane), Anal. Chem. 70 (1998) 4974–4984, https://doi.org/10.1021/ac980656z.
[27] P. de Haan, K. Mathwig, L. Yuan, B.W. Peterson, E. Verpoorte, Facile fabrication of microperforated membranes with re-useable SU-8 molds for organs-on-chips, Organs-on-a-Chip 5 (2023) 100026, https://doi.org/10.1016/j.ooc.2023.100026.
[28] D. Huh, H.J. Kim, J.P. Fraser, D.E. Shea, M. Khan, A. Bahinski, et al., Microfabrication of human organs-on-chips, Nat. Protoc. 8 (2013) 2135–2157, https://doi.org/10.1038/nprot.2013.137.

Dr. Pim de Haan is a postdoctoral fellow in the Pharmaceutical Analysis Group, Groningen Research Institute of Pharmacy, University of Groningen. He received his BSc and MSc degrees in Pharmacy from the University of Groningen, where he obtained his PhD in analytical chemistry in 2021. He is now a postdoctoral fellow in the group of Prof. Sabeth Verpoorte. His research focuses on the design and development of organ-on-a-chip systems for drug testing, with a focus on their read-out and chemical analysis.

Jean-Paul S.H. Mulder has been a research technician in the Pharmaceutical Analysis Group since 2014. His expertise includes the development of novel analytical or technical equipment, as well as various microfabrication procedures that focus on the ease of use of organs-on-chips and fluidic components for e.g. chromatography.

Prof. Joost C. Lötters is a Science Officer with Bronkhorst High-Tech B.V., in Ruurlo, the Netherlands, where he focuses on the development of highly precise devices for flow measurement and control. He is a part-time professor at Delft University of Technology, Department of Precision and Microsystems Engineering, and at the University of Twente, focusing on microfluidic handling systems. He received his MSc and PhD in Electrical Engineering from the University of Twente.

Prof. Sabeth Verpoorte is an analytical chemist with over 30 years' experience in microfluidics. She has held the chair of Analytical Chemistry and Pharmaceutical Analysis within the Groningen Research Institute of Pharmacy, University of Groningen since 2003. She received her PhD from the University of Alberta in 1990, after which she trained as a postdoctoral fellow in the group of Andreas Manz at Ciba in Basel, Switzerland, and continued as a researcher and group leader at the University of Neuchâtel, Switzerland. Her research includes many aspects of microfluidics, including organs-on-chips as well as microfluidic components and separations.